

1995

Nonlinear temporal diffraction and frequency shifts resulting from pulse shaping in chirped-pulse amplification systems

X Liu

University of Michigan - Ann Arbor

R Wagner

University of Michigan - Ann Arbor

Anatoly Maksimchuk

University of Michigan, tolya@umich.edu

E Goodman

University of Michigan - Ann Arbor

J Workman

University of Michigan - Ann Arbor

See next page for additional authors

Follow this and additional works at: <http://digitalcommons.unl.edu/physicsumstadter>

 Part of the [Physics Commons](#)

Liu, X; Wagner, R; Maksimchuk, Anatoly; Goodman, E; Workman, J; Umstadter, Donald P.; and Migus, A, "Nonlinear temporal diffraction and frequency shifts resulting from pulse shaping in chirped-pulse amplification systems" (1995). *Donald Umstadter Publications*. 96.

<http://digitalcommons.unl.edu/physicsumstadter/96>

This Article is brought to you for free and open access by the Research Papers in Physics and Astronomy at DigitalCommons@University of Nebraska - Lincoln. It has been accepted for inclusion in Donald Umstadter Publications by an authorized administrator of DigitalCommons@University of Nebraska - Lincoln.

Authors

X Liu, R Wagner, Anatoly Maksimchuk, E Goodman, J Workman, Donald P. Umstadter, and A Migus

Nonlinear temporal diffraction and frequency shifts resulting from pulse shaping in chirped-pulse amplification systems

X. Liu, R. Wagner, A. Maksimchuk, E. Goodman, J. Workman, D. Umstadter, and A. Migus*

Center for Ultrafast Optical Science, University of Michigan, 2200 Bonisteel Boulevard, Ann Arbor, Michigan 48109-2099

Received January 30, 1995

We present experimental results of the amplification of strongly amplitude-modulated chirped pulses resulting from the coherent addition of two delayed short pulses. The nonlinearities in the amplifier chain induce a temporal diffraction resulting in prepulses and postpulses, in addition to the two main pulses when compressed. Simultaneously, temporal-resolved and spectral-resolved output pulses show that the prepulses and postpulses are blue shifted and red shifted, respectively, explaining the causality of the system.

Pulse shaping has received considerable attention for manipulating ultrashort pulses.¹ It includes the means of generating a train of pulses of variable delay, intensity, and phase from a single short pulse of broad spectrum. One simple shaper consists of two pulses with a variable delay. This can be done in a Michelson interferometer-type delay line. More sophisticated pulse shapers use a zero-dispersion grating-pair stretcher, with an amplitude and phase mask placed in the spectral plane. Currently, in most cases the pulse shaper is linear, i.e., the amplitude and/or phase masks do not depend on the intensity of the pulse, and no nonlinear effect is introduced into the pulses. Pulse-shaping techniques can provide pulses for experiments in which specific pulse shapes with definite pulse delay, amplitude, and phase are required.^{1,2} Although many experiments can use pulses directly from a linear pulse shaper, further amplification is desirable either to get a filtering process to get rid of the spatial nonuniformities introduced by the zero-dispersion devices or to reach higher power levels.³ In this case nonlinear optical effects may play an important role in the output pulses.

Recently nonlinear pulse shapers—the ones in which the pulse-shaping effect is a function of the laser intensity—have been demonstrated.^{4,5} It was shown that when instantaneous nonlinearities are included, unexpected prepulses and postpulses, in addition to the pulses that result from linear pulse shaping, will appear. However, the origin of the additional pulses was not very intuitive⁴ or even invoked noncausal photon echos.⁵ In this Letter we report nonlinear pulse shaping by two chirped pulses propagating in a laser gain medium. The unique feature of our experiment is that we simultaneously resolve temporal and spectral behavior of the pulses using a spectrometer–streak camera combination. We show that additional frequencies are generated as a result of nonlinear interaction in the gain medium and the pulses that carry the new frequencies are those created by temporal diffraction as a result of pulse shaping. We show that this is necessarily true for this type of pulse shaping and explain how causality is taken into account.

The experimental setup is shown in Fig. 1. Two 400-fs laser pulses with a variable delay between them were created with a Michelson interferometer

arrangement. The delay setup was inserted before the stretcher of a chirped-pulse amplification high-power laser system operating at 1.053 μm . The time delay could be varied between 0 and 1200 ps. The laser pulses were then stretched to 950 ps in a grating-pair stretcher. The stretched pulses were amplified in a Ti:sapphire regenerative amplifier and a series of single-pass Nd:glass power amplifiers. The amplified pulses were then compressed back to short pulses by a grating-pair compressor. In our experiment the maximum output was limited to approximately 500 mJ per pulse before compression.

The output pulses were sent to a streak camera coupled to a spectrometer. Figure 2(a) shows the streak camera image when the two pulses from the Michelson interferometer were separated by approximately 1 ns. The streak image shows two compressed pulses. When the time delay was changed to 400 ps, the streak image shows two more pulses, one advanced and one retarded relative to the two initial pulses. The time separations of the four pulses are the same, 400 ps. Furthermore, the observed spectra of the two additional pulses appear narrower, the leading one blue shifted and the trailing one red shifted from the initial pulses, as shown in Fig. 2(b).

The most intuitive way to understand the frequency shift and temporal diffraction is to consider it as a four-wave mixing (FWM) process. As shown in Fig. 1, at any particular position in the overlapped part of the

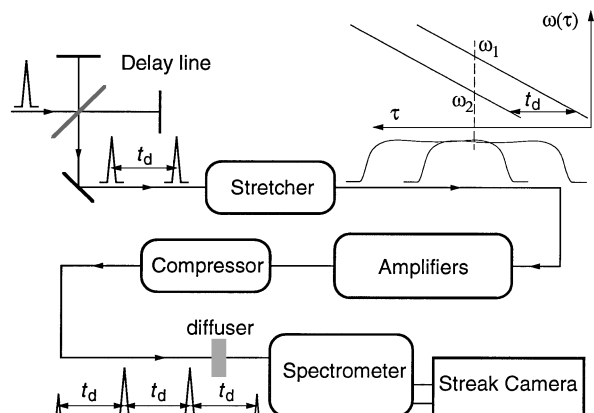


Fig. 1. Experimental arrangement of nonlinear pulse shaping in a chirped-pulse-amplification amplifier.

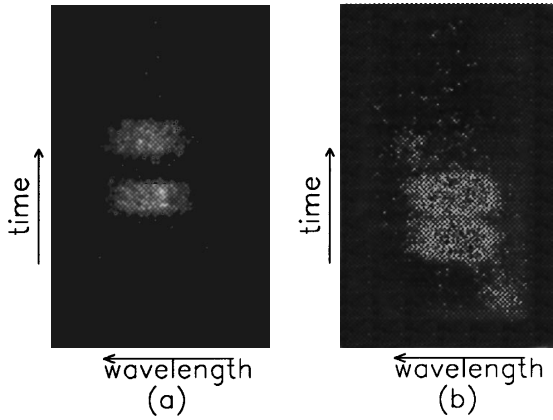


Fig. 2. Spectrally and temporally resolved images of output pulses. The broad pulse widths are due to scattering from a diffuse surface. (a) Pulse separation is 1 ns and the stretched pulses do not overlap in the amplifiers. (b) Pulse separation is 400 ps and the stretched pulses partially overlap in the amplifiers.

two pulses the instantaneous optical carrier frequencies are ω_1 and ω_2 ($\omega_1 > \omega_2$). The instantaneous carrier frequencies of the two chirped pulses are $\omega_1(\tau) = \omega_0 + b(\tau + t_d/2)$ and $\omega_2(\tau) = \omega_0 + b(\tau - t_d/2)$, where t_d is the relative delay. The frequency difference is then $\delta\omega = \omega_1 - \omega_2 = bt_d$.

The third-order nonlinear polarization,

$$P_{NL} = \chi^{(3)}[E_1(\omega_1) + E_2(\omega_2)][E_1^*(-\omega_1) + E_2^*(-\omega_2)] \times [(E_1(\omega_1) + E_1(\omega_1))], \quad (1)$$

gives FWM, self-phase modulation (SPM), and cross-phase modulation (XPM). In particular, the terms $E_1(\omega_1)E_2^*(-\omega_2)E_1(\omega_1)$ and $E_2(\omega_2)E_1^*(-\omega_1) \times E_2(\omega_2)$ are the FWM processes of interest, giving the new frequencies $2\omega_1 - \omega_2$, and $2\omega_2 - \omega_1$. We see that $(2\omega_1 - \omega_2)_\tau = \omega_1 + bt_d$, so it is constantly blue shifted from $\omega_1(\tau)$. Likewise, $2\omega_2 - \omega_1 = \omega_2 - bt_d$ is red shifted from $\omega_2(\tau)$. The FWM process is efficient because it is phase matched because the new frequencies and $\omega_1(\tau)$ and $\omega_2(\tau)$ are all nearly equal. When the chirped pulses are recompressed in the compressor, $\omega_1 + \delta\omega = \omega_1 + bt_d$ is advanced by t_d relative to the ω_1 . Because the unshifted frequencies $\omega_1(\tau)$ collapse to $\tau = 0$ to form the compressed pulse, the blue-shifted frequencies will collapse at $\tau = -t_d$ to form the prepulse. The same applies to the red-shifted postpulse. The partial overlap causes the bandwidth of the new pulses to be narrower, as shown in the experiment. Indeed, no time causality is violated: even though additional pulses appear ahead of the compressed original pulses, they are a result of the new frequencies, and the dispersive properties of the grating compressor and the new pulses fall under the envelope of the chirped pulses. It is clear from the above argument that the additional pulses from such nonlinear shaping arrangements are always blue shifted and red shifted. This should also be the case for the research reported in Refs. 4 and 5. However, in those experiments the delay between the original pulses was small compared with the stretched pulse widths, so the frequency shift $\delta\omega$ was also small and may not be observable. Moreover, the use of a regular

autocorrelator was not suitable for measuring the spectra of individual pulses.

This process of new frequency components giving rise to new pulses is the time-domain analog of spatial nonlinear diffraction. The gist of space-time duality,⁶ is that the temporal equation governing the propagation in a dispersive medium of a pulse with a narrow $\Delta\omega$ spread and spatial propagation in vacuum for a beam of narrow Δk spread have the same form. When two noncollinear and diverging beams overlap spatially in a nonlinear medium, a beat pattern forms. New spatial k vectors ($2\mathbf{k}_1 - \mathbf{k}_2$, $2\mathbf{k}_2 - \mathbf{k}_1$) will be generated as a result of nonlinear interaction in the medium. The new k vectors will give rise to new spots when the pulses are going backward (the compressor analog) on both sides of the initial beam.

Another valid approach is to look at the process as nonlinear propagation of the composite pulse, which contains the beat pattern. The propagation can be described by

$$\frac{\partial A(z, \tau)}{\partial z} = \frac{\gamma}{2} A(z, \tau) - i \frac{\beta''}{2} \frac{\partial A(z, \tau)}{\partial \tau} + i \frac{k_0 n_2}{2} |A(z, \tau)|^2 A(z, \tau), \quad (2)$$

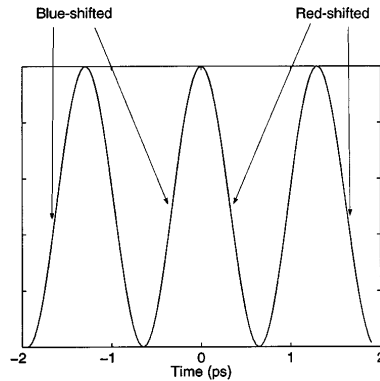


Fig. 3. Temporal beat pattern of the two chirped pulses with a delay $t_d = 400$ ps. Blue-shifted and red-shifted frequencies are generated on the rising and falling sides of the sinusoidal curve.

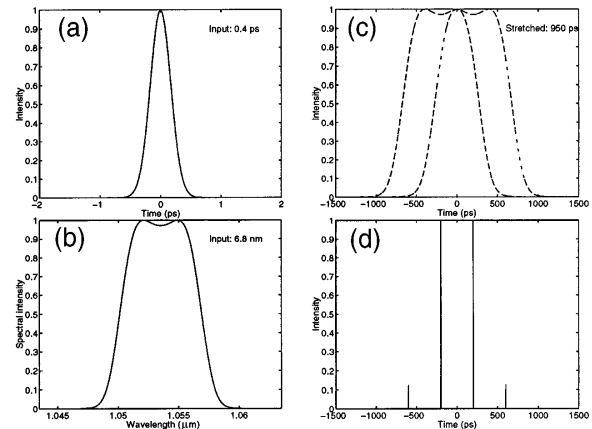


Fig. 4. Simulation example with $B = 0.3$. (a) Input short pulse, (b) input spectrum, reproducing the experimental spectrum, (c) stretched pulses with delay $t_d = 400$ ps, (d) recompressed pulses after propagating in a nonlinear medium.

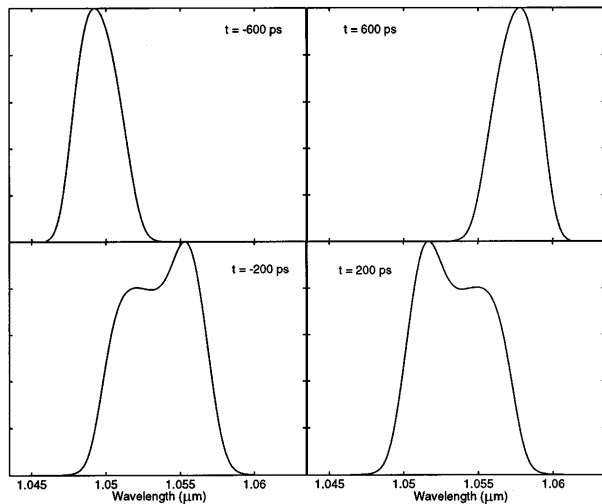


Fig. 5. Spectra of individual recompressed pulses showing the spectral shifts. Note that the spectra of the two original pulses show asymmetric depletion because of the partial overlap of the stretched pulses in the nonlinear medium.

where $\tau = t - z/v_g$, v_g is the group velocity, $\beta'' = \partial^2 k / \partial \omega^2$ is the group-velocity dispersion, γ is the laser gain, $k_0 = n_0 \omega_0 / c$, ω_0 is the central carrier frequency of the pulse, and n_0 is the linear index of refraction. In the amplifiers we ignore the group-velocity dispersion for simplicity ($\beta'' = 0$). γ contains the nonlinearity that is due to gain saturation. Note that the nonlinear phase term $|A(z, \tau)|^2 A(z, \tau)$ contains all the FWM, SPM, and XPM terms; therefore Eq. (2) contains the FWM discussed above. In this picture the new frequencies are generated as a result of SPM, $\delta\omega \propto dI(\tau)/d\tau$. Because of the many rapid intensity oscillations that are due to the beating, as shown in Fig. 3, new frequencies are generated efficiently even though the intensity is not high. All the new frequencies generated this way will interfere in the compressor to give the additional pulses.

To verify this picture and compare it with our experiment, we have conducted numerical integration of Eq. (2). Because the spectrum of the pulse was not Gaussian experimentally, we first obtain a similar spectrum, shown in Fig. 4(b), by sending a 400-fs FWHM Gaussian pulse [Fig. 4(a)] through a nonlinear medium. The pulse is then stretched to 950 ps. The pulse is now split into two: $A(z, \tau) \rightarrow A(z, \tau - t_d/2) + A(z, \tau + t_d/2)$ [Fig. 4(c)]. In the absence of gain saturation, the laser intensity $I(z, \tau) = |A(z, \tau)|^2$ is amplified in the amplifier as $I(z, \tau) = I_{in} e^{\gamma z}$, and the effect of nonlinearity can be expressed by the value of the B integral:

$$B = \frac{2\pi n_2}{\lambda} \int_0^L I(z, \tau) dz = \frac{2\pi n_2}{\lambda} \frac{I_{in} e^{\gamma L}}{\gamma} = \frac{2\pi n_2}{\lambda} \frac{I_{out}}{\gamma}, \quad (3)$$

where L is the length of the gain medium. From Eq. (3) we see that the effective length of the nonlinear medium is $1/\gamma$ for a constant intensity of I_{out} for a laser amplifier. The B integral of the regenerative amplifier is estimated to be $B_{regen} \approx 0.2$. The max-

imum B value of the amplifiers used in the experiment is estimated to be $B_{amp} \approx 0.2$ as well. We can then choose appropriate constant laser intensities I_0 and interaction lengths L for Eq. (2) to yield the same B integral and hence the same nonlinear effect on the pulses, and the gain term is eliminated for simplicity.

In our numerical example shown in Fig. 4 we use $B = 0.3$. The relative delay is $t_d = 400$ ps for Fig. 4(c). Figure 4(d) shows the recompressed pulses with the additional prepulses and postpulses. All four pulses are separated by the initial delay, 400 ps. The energy contained in the prepulses and postpulses is more than 10% of that of the main pulses, showing the efficiency of the nonlinear process. Figure 5 shows the spectra of individual pulses, displaying the spectral shifts and narrower bandwidths discussed above. Another simulation run done for a relative delay of 1000 ps still shows additional prepulses and postpulses with correspondingly larger frequency shifts, but their intensities are too small to be seen on linear scale plots. Nonlinearities caused by gain saturation is also considered in the numerical calculation, resulting in prepulses and postpulses as well. However, the intensity of the additional pulses is approximately 8 orders of magnitude smaller than the original pulses. Therefore we attribute the nonlinearity solely to the instantaneous third-order susceptibility.

In summary, we have demonstrated that the amplification of a strongly amplitude-modulated chirped pulse leads to new prepulses and postpulses when the pulse is compressed, even though a B integral of 0.3 is low for an amplifier system. This result is of general interest for the amplification of shaped pulses because it sets some limits on the allowed high-frequency amplitude modulation on the spectrum where feasible phase manipulation is preferable.⁷ On the other hand, this suggests that this simple type of nonlinear pulse shaping generating a sequence of pulses may find direct applications for plasma Wakefield accelerators, as recently proposed.³

This work was partially funded by the National Science Foundation Center for Ultrafast Optical Science, contract PHY8920108.

*Permanent address, Laboratoire d'Optique Appliquée, Centre National de la Recherche Scientifique URA 1406, ENSTA-Ecole Polytechnique, 91120 Palaiseau, France.

References

1. J. P. Heritage, A. M. Weiner, and R. N. Thurston, *Opt. Lett.* **10**, 609 (1985).
2. A. M. Weiner, J. P. Heritage, and E. M. Kirchner, *J. Opt. Soc. Am. B* **5**, 1563 (1988).
3. D. Umstadter, E. Esarey, and J. Kim, *Phys. Rev. Lett.* **72**, 1224, (1994).
4. M. K. Jackson, G. R. Boyer, J. Paye, M. A. Franco, and A. Mysyrowicz, *Opt. Lett.* **17**, 1770 (1992).
5. V. L. da Silva, Y. Silberberg, and J. P. Heritage, *Opt. Lett.* **18**, 580 (1993).
6. B. Kolner, *IEEE J. Quantum Electron.* **30**, 1951 (1994).
7. J. Paye and A. Migus, "Space-time Wigner functions and their application to the analysis of a pulse shaper," submitted to *J. Opt. Soc. Am. B*.